KNOWLEDGE-BASED SEGMENTATION OF SAR IMAGES

Steven Haker, Guillermo Sapiro and Allen Tannenbaum

University of Minnesota
Minneapolis, MN 55455
{haker,guille,tannenba}@ece.umn.edu

ABSTRACT

A new approach for the segmentation of still and video SAR images is described in this paper. A priori knowledge about the objects present in the image, e.g., *target, shadow,* and *background terrain,* is introduced via Bayes' rule. Posterior probabilities obtained in this way are then anisotropically smoothed, and the image segmentation is obtained via MAP classifications of the smoothed data. When segmenting sequences of images, the smoothed posterior probabilities of past frames are used to learn the prior distributions in the succeeding frame. We show, via a large number of examples from public data sets, that this method provides an efficient and fast technique for addressing the segmentation of SAR data.

1. INTRODUCTION

In this paper we present a novel method of segmenting Synthetic Aperture Radar (SAR) images. The segmentation of SAR data has received an increasing amount of attention from the image processing community in the past years; see for example [2, 3] and references therein.

The SAR images used in this paper are part of a well-known public data set provided jointly by DARPA and Wright Laboratory as part of the Moving and Stationary Target Acquisition and Recognition (MSTAR) program [10]. Figure 1 shows a typical example from the data set. These are images of various military and synthetic targets taken from an airborne platform at various angles. Most of the images are 128 pixels square and are characterized by a graininess that makes direct segmentation of the target difficult. As we show below, the introduction of prior information about the image significantly facilitates the segmentation process.

Since noise is in general non-additive, anisotropic diffusion [4] and related techniques directly applied to the image do not produce satisfactory results. Our approach follows the technique of [7, 8, 9], originally developed for MRI segmentation, and combines Bayes' rule with anisotropic diffusion, introducing a priori knowledge into the segmentation process and solving the non-additivity problem of the noise. We also extend this approach to derive a novel method for the segmentation of video data, incorporating basic learning capabilities to the knowledge.

This work was supported in part by grants from the National Science Foundation ECS-9700588 and NSF-LIS, the Air Force Office of Scientific Research AF/F49620-94-1-00S8DEF, AF/F49620-94-1-0461, AF/F49620-98-1-0168, the Army Research Office DAAH04-94-G-0054, DAAG55-98-1-0169, the Office of Naval Research ONR-N00014-97-1-0509 and Young Investigator Award, and MURI.

2. BASIC MODEL FOR STILL IMAGES

The model we employ begins with the assumption that the image is composed of n classes of objects. For sequences of images, this value n is assumed constant, although this is just a technical limitation introduced mainly to facilitate the discussion. In this paper we will assume three classes, corresponding to the target, its shadow, and the background terrain. The technique is general and can be applied to any number of classes. The goal of our segmentation is to determine to which class each pixel in each image belongs. Our basic model assumes that the value of each pixel in a given class can be thought of as a random variable with a known distribution, and that these variables are independent across pixels. Thus, for the case of normal distributions (see below for extensions), the likelihood of a particular pixel i having a certain value v given that it is in class $c \in \{\text{target}, \text{shadow}, \text{background}\}$ is:

$$\Pr(V_i = v | C_i = c) = \frac{1}{\sqrt{2\pi}\sigma_c} \exp\left(-\frac{1}{2}\frac{(v-\mu_c)^2}{\sigma_c^2}\right) \quad (1)$$

where i is an index ranging over all pixels in the SAR image, V_i is the value of the pixel, and C_i is its class. As usual, μ_c and σ_c denote the mean and standard deviation of class c; these are assumed known. In practice, these parameters are estimated from a set of sample images. When segmenting sequences of images, we have tried relaxing the assumption of normally distributed intensities. This is described below.

Next, we assume that there is some known prior probability that a particular pixel will belong to a certain class. For single-image data sets, we assume a homogeneous prior, i.e., that $\Pr(C_i = c)$ is the same over all spatial indices i. It is, however, possible to incorporate a priori knowledge about the image here, for example if it were known that the target is more likely to be near the center of the image than near the edge. For sequences of images, we have used a learned prior, as described below.

Given a set of intensity distributions $\Pr(V_i = v | C_i = c)$ and priors $\Pr(C_i = c)$, we can apply Bayes' Rule from elementary probability theory to calculate the posterior probability that a given pixel belongs to a particular class, given

0-8186-8821-1/98 $10.00 © 1998 IEEE

its intensity:

$$\Pr(C_i = c|V_i = v) = \frac{\Pr(V_i = v|C_i = c)\ \Pr(C_i = c)}{\sum_\gamma \Pr(V_i = v|C_i = \gamma)\ \Pr(C_i = \gamma)}. \quad (2)$$

Our proposed approach is to calculate the posteriors $P_i^c := \Pr(C_i = c|V_i = v)$ using the given distributions and (2) above, and then to apply anisotropic smoothing to each P^c (note that the denominator is just a normalization constant that can be "ignored"). Specifically, we have chosen to smooth by evolving P^c according to a discretized version of the partial differential equation

$$\frac{\partial P^c}{\partial t} = ((P_y^c)^2 P_{xx}^c - 2P_x^c P_y^c P_{xy}^c + (P_x^c)^2 P_{yy}^c)^{1/3}. \quad (3)$$

This equation defines the affine geometric heat flow, under which the level sets of P^c undergo affine curve shortening. This particular diffusion equation was chosen because of its affine invariance, because it preserves edges well, and because of its numerical stability and ease of computation. See [1, 5, 6] for details and other applications of this filter. Once again, the technique is not limited to any specific selection of the edge preserving filter (e.g., in [7, 8, 9] the original Perona-Malik flow is used for MRI).

The final segmentation is obtained using the maximum *a posteriori* probability estimate after anisotropic smoothing. That is,

$$C_i^* = \underset{c \in \{\text{target, shadow, background}\}}{\arg\max} \Pr^*(C_i = c|V_i = v) \quad (4)$$

where $\Pr^*(C_i = c|V_i = v)$ is the smoothed posterior probability. More details on this technique, and its relation to other approaches such as MRF and relaxation labeling, may be found in [7, 8, 9].

3. EXTENSIONS TO VIDEO DATA

When segmenting sequences of images, we have extended the model so that information from one frame is used in the segmentation of the next one. By far the most effective way we have found to do this is by modifying our assumption of homogeneous priors. In particular, we have learned these priors. We have used the smoothed posteriors P^c from one frame as priors $\Pr(C_i = c)$ in the segmentation of the next frame. We have also tested relaxing our assumption that the pixel intensities are distributed according to fixed normal distributions. We learned the distribution parameters of the normal distributions from frame to frame by calculating new sample means and variances based on the segmentation of earlier images. Finally, we completely removed the assumption that the intensities are normally distributed. This was done by learning the sample distribution of intensities within each class as images were segmented, and then using this distribution as $\Pr(V_i = v|C_i = c)$ in (1) when segmenting succeeding frames.

Recapping, we can learn the distributions from previous frames in the case of video data, or from examples in the case of still images.

4. EXAMPLES

The Wright Laboratories' SAR image data is stored as 4-byte floating point data in separate magnitude and phase blocks. Only the magnitude block was used in our segmentation. The data was scaled to range between 0.0 and 255.0.

In order to get initial estimates for μ_c and σ_c, a few images were segmented by hand. Once areas of each image were identified as either target, shadow, or background, the sample mean and standard deviation of the values of the pixels in these areas were calculated. These values were then used for μ_c and σ_c in (1) and (2). We found that a single set of values for the parameters μ_c and σ_c worked well for many different targets and viewing angles. The values used in the segmentations below were (for still images):

$$(\mu_{target}, \mu_{shadow}, \mu_{background}) = (61.7, 1.6, 7.8) \quad (5)$$

$$(\sigma_{target}, \sigma_{shadow}, \sigma_{background}) = (53.7, 0.8, 4.3) \quad (6)$$

Next, values for $\Pr(C_i = c)$ were chosen. We have found that the segmentation process is quite robust with respect to these values. In fact, $\Pr(C_i = c) \equiv \frac{1}{3}$ provided satisfactory results. However, when segmenting sequences of images, significant gains in speed are possible through the use of adaptive priors, as described above.

To segment a singular image, the data was read and scaled. The image itself was then smoothed directly by applying (3) for a small number of iterations, typically three. Next, the posterior probabilities were calculated using (1) and (2), and the parameter estimates (5),(6) above. The posterior probabilities P^c were then smoothed using (3) for a number of iterations. After each iteration, the three probabilities P^c were renormalized so that their sum was one. Ten iterations was the average number required to produce a good result. Whenever (3) was applied, the maximum time step which ensures numerical stability was used. The final step in the calculation was to use (4) to determine the class of each pixel. The results were saved as images so that they could be compared visually to the original. These results are shown below in figures (1)-(8). For all of these segmentations, (3) was applied three times to the original image and ten times to the posterior probabilities.

To segment a sequence of images, the first image in the sequence was segmented as above. The smoothed posterior probabilities P^c were then used as prior probabilities in the segmentation of the second image, and similarly for all succeeding images. As with singular images, sequences of segmented results were saved as images. The results are given below in figures (9) through (16), along with the prior probabilities used in segmenting each frame. For all of these segmentations, (3) was applied two times to the original image and to the posterior probabilities as well. The small amount of smoothing needed makes the average per-frame segmentation time significantly smaller than the average time required to segment still images. Note that the amount of residual noise in the segmentation drops from frame to frame. By the tenth image, the speckles in the segmentation have practically disappeared. We could have smoothed the earlier frames more to remove this noise, but we have smoothed all frames equally here to show how the segmentation improves as the prior adapts.

We also tried using adaptive intensity distributions from frame to frame. We did this by calculating new sample means and variances μ_c and σ_c based on the segmentations of earlier images. As a further generalization, we tried relaxing the assumption of normally distributed intensities. This was done by keeping track of the actual distribution of intensities within each segmented class as frames were processed, and then using this distribution as $\Pr(V_i = v|C_i = c)$ in (1) when segmenting succeeding frames. In general, we did not see a marked improvement over the static distribution model when using either of these methods. We believe that this is another indication that our basic method is robust.

5. CONCLUDING REMARKS

In this paper we have used the technique introduced in [7] for the segmentation of SAR data. We also extended this general approach to the segmentation of video data. The result is a fast and reliable algorithm that segments SAR data based both on prior and learned information.

Simple prior distributions and adaptation techniques were used in this paper, since the results obtained were already satisfactory. For more difficult data, it is possible to introduce more sophisticated multi scale texture models for the likelihood of the background. Another possible extension will be to consider that n, the number of classes in the image, is not given and needs to be estimated as well. This can be done for example via EM type algorithms. Note although that since the scheme here described is extremely fast, especially for video data were the number of smoothing steps is dramatically reduced, a brute-force search for n in a given range might be good enough for a number of applications.

6. REFERENCES

[1] L. Alvarez, F. Guichard, P. L. Lions, and J. M. Morel, "Axioms and fundamental equations of image processing," *Arch. Rational Mech. Anal.*, 123 (1993), p.3.

[2] C. H. Fosgate, H. Krim, A. S. Willsky, and W. C. Karl, "Multiscale segmentation and anomaly enhancement of SAR imagery," *Proc. IEEE ICIP*, 1996.

[3] J. C. Lee and D. C. Munson, Jr., "Runway imaging from an approaching aircraft using synthetic aperture radar," *Proc. IEEE ICIP*, 1996.

[4] P. Perona and J. Malik, "Scale-space and edge detection using anisotropic diffusion," *IEEE-PAMI* **12**, pp. 629-639, 1990.

[5] G. Sapiro and A. Tannenbaum, "Image smoothing based on an affine invariant flow," *Proceedings of Conference on Information Sciences and Systems*, Johns Hopkins University, Baltimore, Maryland, March 1993, pp.196-201.

[6] G. Sapiro and A. Tannenbaum, "On affine plane curve evolution," *Journal of Functional Analysis* **119:1**, pp. 79-120, January 1994.

[7] P. Teo, G. Sapiro, and B. Wandell, "Creating connected representations of cortical gray matter for functional MRI visualization," *IEEE Trans. Medical Imaging*, December 1997.

[8] P. Teo, G. Sapiro, and B. Wandell, "Anisotropic diffusion of posterior probabilities," *Proc. IEEE-International Conference on Image Processing*, Santa Barbara, California, October 1997.

[9] P. Teo, G. Sapiro, and B. Wandell, "Anatomically consistent segmentation of the human cortex for functional MRI visualization," *International Conference on Computer Vision*, Bombay, India, January 1998.

[10] "MSTAR Targets T-72, BMP-2, BTR-70, SLICY," Veda Incorporated, Dayton, Ohio, 1997 (Public CDROM). Also available at www.mbvlab.wpafb.af.mil/public/MBVDATA.

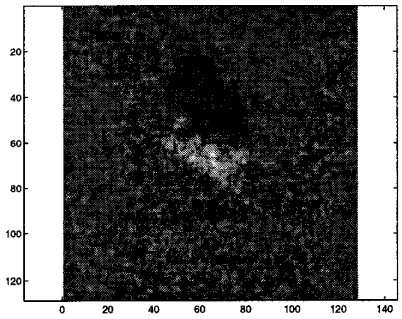

Figure 1: Typical SAR Image - A Tank

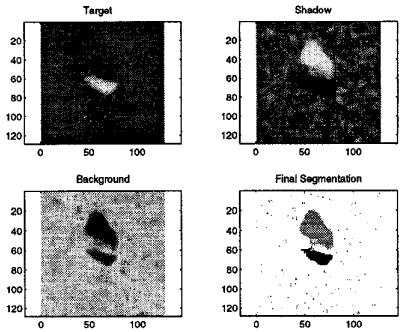

Figure 2: Smoothed Posteriors and Segmentation of Figure 1.

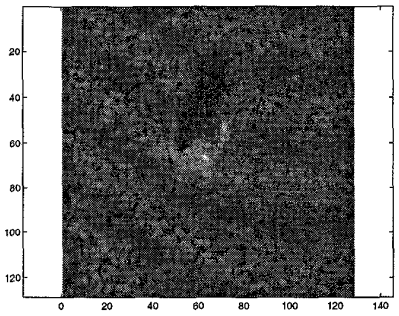

Figure 3: Armored Personnel Carrier

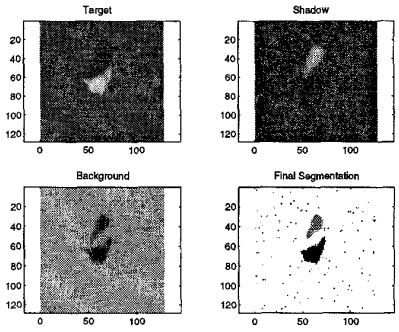

Figure 4: Smoothed Posteriors and Segmentation of Figure 3.

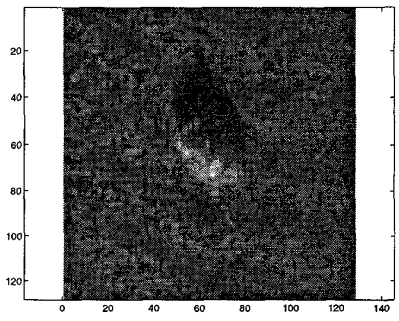

Figure 5: Second Tank

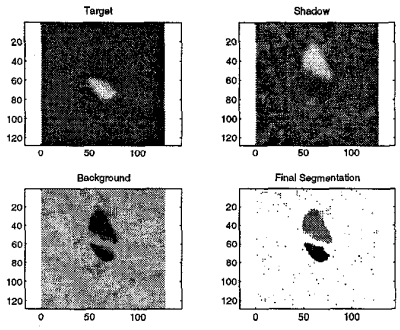

Figure 6: Smoothed Posteriors and Segmentation of Figure 5.

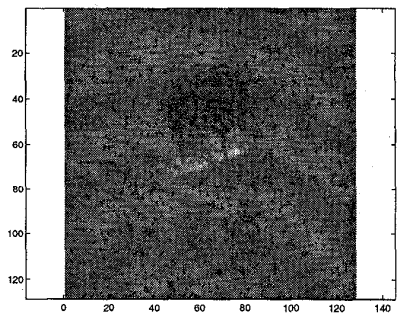

Figure 7: Second Personnel Carrier

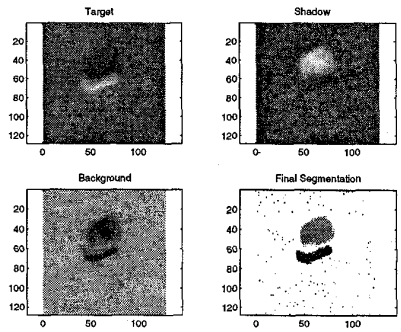

Figure 8: Smoothed Posteriors and Segmentation of Figure 7.

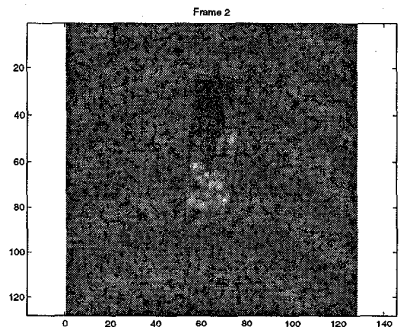

Figure 9: Video Sequence Frame 2

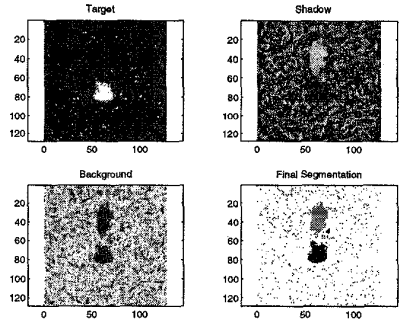

Figure 10: Priors and Final Segmentation of Figure 9

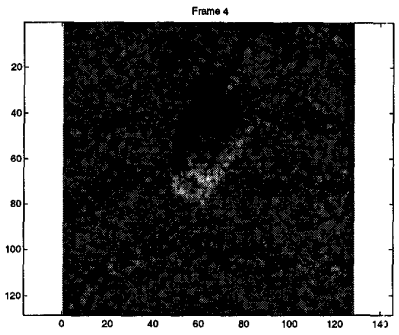

Figure 11: Video Sequence Frame 4

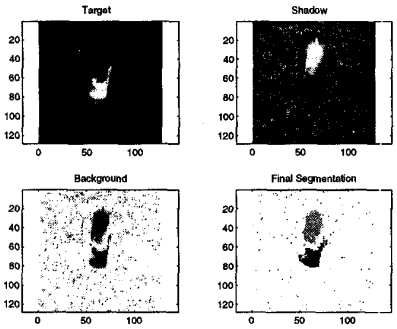

Figure 12: Priors and Final Segmentation of Figure 11

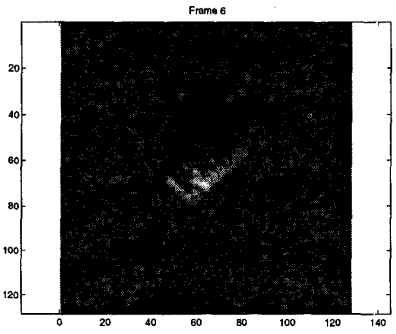

Figure 13: Video Sequence Frame 6

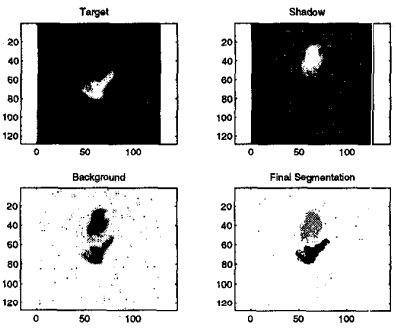

Figure 14: Priors and Final Segmentation of Figure 13

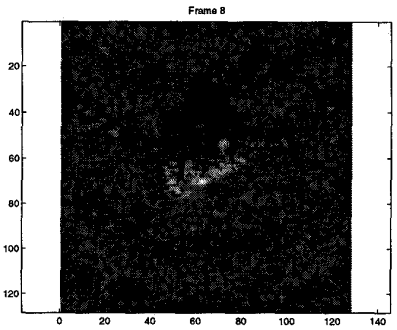

Figure 15: Video Sequence Frame 8

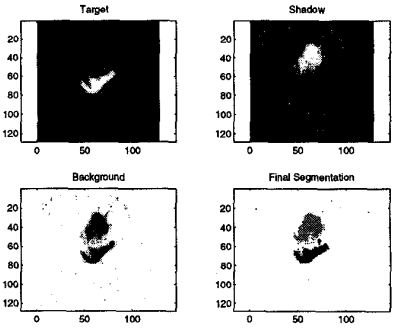

Figure 16: Priors and Final Segmentation of Figure 15